# AUTOMATIC VESSEL TREE STRUCTURE EXTRACTION BY GROWING MINIMAL PATHS AND A MASK

*Da Chen and Laurent D. Cohen*

CEREMADE, UMR 7534, Université Paris Dauphine, 75775 Paris Cedex 16, France

## ABSTRACT

In this paper, we propose a completely automatic method to extract the vessel tree structure including its centerlines and radius using geodesic paths technology. Our main goal is to find a set of key points located in the vessel centerlines, link each pair of key points by minimal paths for finding the vessels between them and stop this process automatically. This work adapts the growing minimal paths method to find the set of key points. The main drawback of growing minimal paths is when to stop the processing. To solve this problem we propose an automatic stopping criteria. Additionally, we use a cake wavelet to compute the vessel measurement consisting of both radius and orientation to develop the classical growing minimal paths model which cannot guarantee the extracted tree corresponds to the centerlines of the vessel tree.

***Index Terms***— Vessel extraction, key points, growing minimal paths, isotropic fast marching.

## 1. INTRODUCTION

Energy minimization techniques have been widely applied to solve various problems in image processing and computer vision. Minimal paths model is one of the most successful applications of energy minimization. Since the seminal work of L.Cohen et al. [1], minimal paths model has been extensively used for vessel tree extraction due to the advantages of the minimal paths methods like global minimizers, fast computation and robustness to noise. In order to extract the vessel centerline and surfaces simultaneously, Li et al.[2] proposed a variant of the purely spatial minimal path technique by incorporating an extra radius dimension into the vessel space. In the 3D paths, each point consists of both the spatial coordinates and an additional radius dimension. This third dimension can describe the vessel thickness at the corresponding 2D point. Taking into account of the orientation information, M. Péchaud et al. [3] incorporated an extra orientation dimension into [2]. With the enhancement of extra-orientation, this model can give better results than the original Li's model. As the classical minimal paths model[1] needs precise information of endpoints, a novel minimal path approach proposed by F. Benmansour et al.[4] to find a set of key points iteratively in the curves (2D) or surfaces (3D) with less restrictive prior knowledge. In this method, user can provide only a single point. The keypoints-based growing minimal paths model (KPGMM) has a good performance in closed curves detection. But for open curves, the KPGMM requires a user-given total length of the curves. V. Kaul[5] gave a new stopping criterion to automatically stop the FM processing and also proposed a new method to compute the paths length. However, both [1] and [5] are only applied to spatial curve detection. For tubular structure extraction, [6] use keypoints searching strategy with radius + 2D spatial location. In this paper, we use both radii and orientation dimension.

In this paper, we present a method to extract the vessel tree structure without any a priori knowledge. This method is based on the classical KPGMM with extra radii and orientation Dimensions. We construct the 4D potential by the orientation score computed by the cake wavelet [7, 8] and then launch the isotropic Fast Marching method (FMM) to get the geodesic distance and length map simultaneously. The main issue is how to stop the set of key points. Once they have covered the main branches, they go out and can include paths with no interesting meaning. This is why we introduce the use of mask. A mask is incorporated into the key points searching scheme to stop the FMM processing. This allows an automatic and efficient definition of the set of keypoints, leading a precise segmentation of the vascular tree.

## 2. BACKGROUND

### 2.1. Minimal Paths Model

Given a 2D image $I : \Omega \to \mathbf{R}^+$ and two points $\mathbf{p_1}$ and $\mathbf{p_2}$, a crucial step of the minimal paths [1] is to build a potential $\mathcal{P} : \Omega \to \mathbf{R}^+$ with lower values near the features. The minimal paths model is formulated to find geodesic paths $\gamma$ to minimize the following energy functional $E : \mathcal{A}_{\mathbf{p_1},\mathbf{p_2}} \to \mathbf{R}^+$:

$$E(\gamma) = \int_\gamma (\mathcal{P}(\gamma) + w)ds = \int_\gamma \widetilde{\mathcal{P}}(\gamma)ds \qquad (1)$$

Where $\mathcal{A}_{\mathbf{p_1},\mathbf{p_2}}$ is the set of all paths linking $\mathbf{p_1}$ and $\mathbf{p_2}$, $s$ is the arc-length parameter and $w$ is a positive constant. A minimal path can be defined as a curve connecting $\mathbf{p_1}$ and $\mathbf{p_2}$ that globally minimizes the energy (1). The solution of this optimization problem is obtained through the computation of the minimal action map $\mathcal{U} : \Omega \to \mathbf{R}^+$. The minimal action map is the minimal energy integrated along a path between $\mathbf{p_1}$ and any point $\mathbf{x}$ of the domain $\Omega$:

$$\mathcal{U}(\mathbf{x}) = \min_{\gamma \in \mathcal{A}_{\mathbf{p_1},\mathbf{x}}} \int_\gamma \widetilde{\mathcal{P}}(\gamma) ds, \quad \forall \mathbf{x} \in \Omega \tag{2}$$

And $\mathcal{U}$ satisfies the Eikonal equation:

$$\begin{cases} \|\nabla \mathcal{U}\| = \widetilde{\mathcal{P}}(\gamma) & \forall \mathbf{x} \in \Omega \\ \mathcal{U}(\mathbf{p_1}) = 0 \end{cases} \tag{3}$$

The minimal path $\mathcal{C}_{\mathbf{p_1},\mathbf{p_2}}$ can be tracked by:

$$\begin{cases} \mathcal{C}'(s) = -\nabla \mathcal{U} \\ \mathcal{C}_{\mathbf{p_1},\mathbf{p_2}}(\mathbf{p_1}) = 0 \end{cases} \tag{4}$$

The Euclidean path length map $\mathcal{L} : \Omega \to \mathbf{R}^+$, is the length of minimal path $\mathcal{C}_{\mathbf{p_1},\mathbf{x}}$, where $\mathbf{x}$ is any point in the image domain $\Omega$. Solving the Eikonal equation (3), [1] adapts the FMM (for details of FMM, refer to [5, 9]).

### 2.2. Classical KPGMM

Among all points in the front of the Fast Marching (FM) propagation which have the same minimal action map values, a point is likely to be located on the curve (2D) or surface(3D) if this point has the largest Euclidean path length map value. Specifically, when the front of the FM propagates to the first point whose Euclidean path length map value exceeds the given threshold $\lambda \in \mathbf{R}^+$, this point is selected as keypoint. Keypoints are iteratively detected until the stopping criterion is statified. See [4, 5] for mare details.

## 3. A MASK BASED GROWING MINIMAL PATHS WITH EXTRA RADII AND ORIENTATION

### 3.1. Orientation Score based 4D Potential

For a given image $I : \Omega \to \mathbf{R}^+$ an orientation score[8, 11] $\Im : \Omega \times \mathrm{S}^1$ of $I$ can be computed by convolution with a mutil-directional wavelet $\psi_\theta$:

$$\Im(\mathbf{x}, \hat{\theta}) = I(\mathbf{x}) * \bar{\psi}_{\hat{\theta}}(-\mathbf{x}) \tag{5}$$

Where $\bar{\psi}_{\hat{\theta}}$ is complex conjugate of $\psi_{\hat{\theta}}$. $\hat{\theta} \in [0 \ \ 2\pi]$ is the orientation variable. We adapt the cake wavelet [7, 8, 11] as the multi-directional wavelet. The cake wavelet is constructed from the Fourier domain (by using polar coordinates):

$$\widehat{\psi}^{\mathrm{cw}}_{\hat{\theta}}(\omega) = \begin{cases} B_k\Big(\frac{\hat{\theta} \mod 2\pi - \frac{\pi}{2}}{2\pi N^{-1}}\Big)\mathcal{M}_m(p), & if \quad p > 0 \\ \frac{1}{N}, & if \quad p = 0 \end{cases} \tag{6}$$

Where $N$ is the number of orientations, $\omega = (p\cos\hat{\theta}, p\sin\hat{\theta})$ and $B_k$ is the $k$-th order B-Spline function. The function

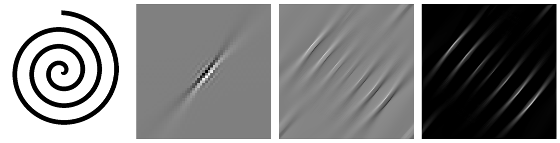

**Fig. 1**. Steps of the Potential construction (see text).

$\mathcal{M}_m(p) = e^{-p}\sum_{k=0}^{m} \frac{p^k}{k!}$. The cake wavelet in spatial domain can be obtained by:

$$\psi_{\hat{\theta}}(\mathbf{x}) = \mathcal{F}^{-1}\Big(\widehat{\psi}^{\mathrm{cw}}_{\hat{\theta}}\Big)(\mathbf{x}) G_\sigma(\mathbf{x}) \tag{7}$$

with $G_\sigma(\mathbf{x})$ is a Gaussian kernel. We only utilize the imaginary part of the orientation score[8, 11]:

$$\Im_{\hat{\theta}}(\mathbf{x}) = Imag\{I * \psi^{cw}_{\hat{\theta}}\}(\mathbf{x}) \tag{8}$$

In order to perform a 4D isotropic Fast Marching propagation with extra radii, we construct the 4D potential $\mathcal{P} : \Omega \times S^1 \times \Re^1 \to \mathbf{R}^+$ as follows:

$$\overline{\mathcal{P}}(\mathbf{x}, \theta, r) = \Big\{\hbar(r) \cdot (\Im_\theta * \mathcal{Q}_{\theta-\pi/2,r})\Big\}(\mathbf{x}) \tag{9}$$

$$\begin{cases} \mathcal{P}(\mathbf{x}, \theta, r) = \alpha\big(\overline{\mathcal{P}} + |\overline{\mathcal{P}}| + c_0\big)^{-1} + c & \text{(10a)} \\ \mathcal{P}(\mathbf{x}, \theta, r) = \alpha\big(\overline{\mathcal{P}} - |\overline{\mathcal{P}}| + c_0\big)^{-1} + c & \text{(10b)} \end{cases}$$

Where $\mathbf{x} \in \Omega$ is a pixel position, $\theta \in [\frac{1}{2}\pi \ \ \frac{3}{2}\pi]$ is the orientation variable(As $\Im_\theta = -\Im_{\theta+\pi}$, we use $\theta \in [0 \ \ \pi]$ ), and $r \in [0 \ \ r_{max}]$ is the radii variable ($r_{max}$ is the largest radius given by the user). $\hbar(r)$ is a weighted function. $\alpha$, $c_0$ and $c$ are positive constants depending on the images. $\mathcal{Q}_{\theta,r}$ can be computed in the polar coordinates:

$$\mathcal{Q}_{\theta,r}(\varpi) = \begin{cases} e^{\frac{-(\theta-\theta_0)^2}{\sigma_1^2}} \cdot e^{\frac{-(r-r_0)^2}{\sigma_2^2}}, & \theta \in [0 \ \ \pi] \\ -e^{\frac{-(\theta-\theta_0)^2}{\sigma_1^2}} \cdot e^{\frac{-(r-r_0)^2}{\sigma_2^2}}, & \theta \in (\pi \ \ 2\pi] \end{cases} \tag{11}$$

Where $\varpi = (r_0\cos\theta_0, r_0\sin\theta_0)$. $\sigma_1$ and $\sigma_2$ are positive constants.In this paper we set that $\sigma_1 = 0.01$ and $\sigma_2 = 0.1$. In Fig.1 we show this course of potential construction. For two boundaries of a vessel, the orientation score value will be positive in one boundary and negative in another one depending on the gray level of the vessels and the background. Therefore, if the gray values in the vessel are lower than that in background, we use $(10a)$, otherwise use $(10b)$. Fig.1(a) is a synthetic Spiral with width 8, (b) is a cake wavelet in spatial domain with a orientation $\theta = \frac{6}{N} \times 2\pi$ ($N = 36$). (c) is the orientation score obtained by the cake wavelet shown in (b). (d) shows the potential obtained by (10a) with $r = 8$.

### 3.2. Mask-based 4D growing minimal paths and stopping criterion

In this paper, we propose a mask based growing minimal paths method to automatically stop the propagation. The motivation of the use of mask is that after the keypoints detected by classical KPGMM have covered the main branches, they will go out and lead to some paths without meaning. With a mask, the set of keypoints will be re-defined automatically and efficiently to obtain more precise segmentation results. Also a positive threshold factor $T$ can be used together with the mask to stop the FM propagation automatically (see section 4.1 for details of the mask).

#### 3.2.1. Steps of 4D the keypoints searching scheme

Let $N_8(\mathbf{p})$ denote the set of 8 neighbours of a 4D point $\mathbf{p}$. Set minimal action map $\mathcal{U} = +\infty$ and path length map $\mathcal{L} = +\infty$ for each point. Select the pixel $\mathbf{p}_0$ with minimum of the Potential $\mathcal{P}$ as the source point, set $\mathcal{U}(\mathbf{p}_0) = 0$ and $\mathcal{L}(\mathbf{p}_0) = 0$. Move $\mathbf{p}_0$ to Trial set, and set all other points as Far. For given threshold $\lambda$, threshold factor $T$, mask $\mathbf{M}$, and Potential $\mathcal{P}$, we do the following loops:

***While the Trial Points Set is not empty, do***:
*Find* $\mathbf{p}_{min}$*, the Trial point with the smallest* $\mathcal{U}$.
*If* $\mathcal{L}(\mathbf{p}_0) > \lambda$ *and* $\mathbf{M}(i, j) = 1$:
- set $\mathcal{U}(\mathbf{p}_{min}) = \mathcal{L}(\mathbf{p}_{min}) = 0$;
- tag $\mathbf{p_{min}}$ as a key point and Trial;
- track the geodesic from $\mathbf{p}_{min}$ according to Equ.(4).

*Else if* $\mathcal{L}(\mathbf{p}_0) \leq (\lambda \cdot T)$:
- Tag $\mathbf{p_{min}}$ as Alive;
- For each Non-Alive point $\mathbf{p}_n \in N_8(\mathbf{p}_{min})$, do $\{\mathcal{U}(\mathbf{p}_n), \mathcal{L}(\mathbf{p}_n)\} = UpdateFM$ and Tag $\mathbf{p}_n$ as Trial.

*Else if* $\mathcal{L}(\mathbf{p}_0) > (\lambda \cdot T)$ *and* $\mathbf{M}(i, j) = 0$:
- Stop the FM propagation completely.

***End***

#### 3.2.2. Details of $UpdateFM$

The method $UpdateFM$ can simultaneously compute the minimal action map and path length map for a point $\mathbf{p} = \{i, j, k, l\}$. We note $\{A, A_1\}$, $\{B, B_1\}$, $\{C, C_1\}$ and $\{D, D_1\}$ the four couples of opposite neighbors such that we get the ordering $A \leq A_1, B \leq B_1, C \leq C_1$, $D \leq D_1$ and $A \leq B \leq C \leq D$. $\{A_0,\, B_0,\, C_0,\, D_0\}$ are the corresponding path length map values of the grid points whose minimal action map values are $\{A, B, C, D\}$ respectively. Assume $u = v = 0$, we compute the the discriminant $\triangle_1^{\mathcal{U}}$ and $\triangle_1^{\mathcal{L}}$ of

$$(u - A)^2 + (u - B)^2 + (u - C)^2 + (u - D)^2 = \mathcal{P}^2(\mathbf{p}) \quad (12)$$

$$(v - A_0)^2 + (v - B_0)^2 + (v - C_0)^2 + (v - D_0)^2 = 1 \quad (13)$$

***If*** $\triangle_1^{\mathcal{U}} \geq 0$, we get

$$u = \Big\{(A + B + C + D) + \sqrt{\triangle_1^{\mathcal{U}}}\Big\}/4 \quad (14)$$

$$v = \Big\{(A_0 + B_0 + C_0 + D_0) + \sqrt{\max\{\triangle_1^{\mathcal{L}}, 0\}}\Big\}/4 \quad (15)$$

***If*** $u \leq D$ or $\triangle_1^{\mathcal{U}} \leq 0$, compute $\triangle_2^{\mathcal{U}}$ and $\triangle_2^{\mathcal{L}}$ of

$$(u - A)^2 + (u - B)^2 + (u - C)^2 = \mathcal{P}^2(\mathbf{p}) \quad (16)$$

$$(v - A_0)^2 + (v - B_0)^2 + (v - C_0)^2 = 1 \quad (17)$$

***If*** $\triangle_2^{\mathcal{U}} \geq 0$, we get

$$u = \Big\{(A + B + C) + \sqrt{\triangle_2^{\mathcal{U}}}\Big\}/3 \quad (18)$$

$$v = \Big\{(A_0 + B_0 + C_0) + \sqrt{\max\{\triangle_2^{\mathcal{L}}, 0\}}\Big\}/3 \quad (19)$$

***If*** $u \leq C$ or $\triangle_2^{\mathcal{U}} \leq 0$, compute $\triangle_3^{\mathcal{U}}$ and $\triangle_3^{\mathcal{L}}$ of:

$$(u - A)^2 + (u - B)^2 = \mathcal{P}^2(\mathbf{p}) \quad (20)$$

$$(v - A_0)^2 + (v - B_0)^2 = 1 \quad (21)$$

***If*** $\triangle_3^{\mathcal{U}} \geq 0$, we get

$$u = \Big\{(A + B) + \sqrt{\triangle_3^{\mathcal{U}}}\Big\}/2 \quad (22)$$

$$v = \Big\{(A_0 + B_0) + \sqrt{\max\{\triangle_3^{\mathcal{L}}, 0\}}\Big\}/2 \quad (23)$$

***If*** $u \leq B$ or $\triangle_3^{\mathcal{U}} \leq 0$, we have $u = A + \mathcal{P}(\mathbf{p})$ and $\mathcal{L} = A_0 + 1$. Then $\mathcal{U}(\mathbf{p}) := min\{\mathcal{U}(\mathbf{p}), u\}$, $\mathcal{L}(\mathbf{p}) := min\{\mathcal{L}(\mathbf{p}), v\}$. Tag $\mathbf{p}$ as Trial.

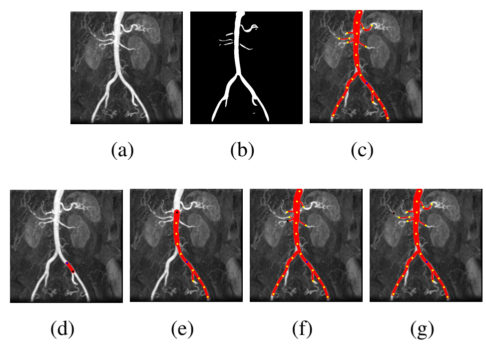


**Fig. 2**. Results (top row) and the course of the proposed method (bottom row, see text).

## 4. EXPERIMENTS

### 4.1. Details of the proposed method

For the mask, many vessel detection methods can be used. In this paper, we choose the Hessian-based[10] model to make a mask. After getting the Hessian-based vessel measurement, we threshold this and obtain a binary mask like Fig.2(b) and Fig.3(b). Fig.2(a) is the original image, (b) is the mask and (c) is the result by our method. We show 4 intermediate results of our method in Fig.2(d)$\sim$(f). In those results, blue points are the source points and black points are the detected key points. Fig.2(g) shows the end point (black point ) for which the propagation stops completely when the front reaches it.

### 4.2. Evaluation on synthetic image

Fig.3 shows an experiment in a synthetic image. (a) is the original image with noise and (b) is the Hessian-based mask.

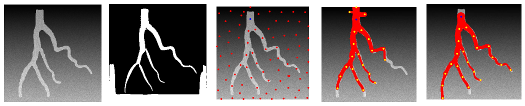

(a) (b) (c) (d) (e)

**Fig. 3**. Results in synthetic image.

**Table 1**. Quantitative evaluation results

| $\lambda$ | $\lambda$ =33 | $\lambda$ =43 | $\lambda$ =53 | Mask | Fig3(d) |
|---|---|---|---|---|---|
| Error | 0.86 | 1.0 | 0.94 | 7.62 | 1.4 |

(c) is the by classical KPGMM. (d) is a part of results of (c) with the same number of keypoints to (e) which is the result of our method: blue point is the source point and yellow points are the keypoints detected ($\lambda = 33$ and $T = 1.2$). In (c) the keypoints are located everywhere after covering the main branches. We compare the results shown in Fig.3 with error defined below in (24). Let $C_g$ be the ground truth contours and $P_i$ be the $i^{th}$ pixel located at the detected boundaries.

$$Error = \frac{1}{N_0} \sum_{i=1}^{N_0} \mathrm{Dis}(C_g, P_i) \tag{24}$$

where $\mathrm{Dis}(C_g, P_i)$ is the minimal distance among all the distances from pixel $P_i$ to each pixel of $C_g$. $N_0$ is the total number of pixels on the detected contours. We compare the results for different thresholds $\lambda$ but with same $T$ in Table 1. Our method can give a better performance as the propagation can be stopped by the criteria to avoid the influence by the noise.

### 4.3. Comparison with the classical KPGMM

In Fig.4 we show two results: (a)a part of results without mask and (b)a part of results (Fig.2 (c)) with mask. Both the yellow points in (a) and (b) inside the green boxes are the thirteenth keypoints with the same spatial location, radii and orientation. Due to the mask-based stopping criteria, the proposed method can avoid taking a point which can be tagged as keypoint by the classical KPGMM (like the black point in (a)) but outside the mask as key point. Instead, the front will continue to propagate until finding a point with length more than $\lambda$ but inside the mask, like the black point in (b). This the main advantages of our method comparing to the classical KPGMM.

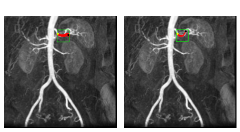

(a) (b)

**Fig. 4**. Parts of segmentation results (see text).

## 5. CONCLUSIONS

We propose an automatic vessel tree extraction method based on a mask and 4D KPGMM . With the orientation score, we construct a 4D potential with extra radii and orientation dimensions. Experiments show our method can get a better performance than the classical KPGMM.

## 6. REFERENCES


[1] L. D. Cohen and R. Kimmel, “Global minimum for active contour models: A minimal path approach,” *International Journal of Computer Vision*, vol. 24, no. 1, pp. 57–78, 1997.

[2] H. Li and A. Yezzi, “Vessels as 4-D curves: Global minimal 4-D paths to extract 3-D tubular surfaces and centerlines,” *IEEE Transactions on Medical Imaging*, vol. 26, no. 9, pp. 1213–1223, 2007.

[3] Michaël Péchaud, Renaud Keriven, and Gabriel Peyré, “Extraction of tubular structures over an orientation domain,” *In CVPR*, pp. 336–342, 2009.

[4] F. Benmansour and L. D. Cohen, “Fast object segmentation by growing minimal paths from a single point on 2D or 3D images,” *Journal of Mathematical Imaging and Vision*, vol. 33, no. 2, pp. 209–221, 2009.

[5] V. Kaul, A. Yezzi, and Yichang Tsai, “Detecting curves with unknown endpoints and arbitrary topology using minimal paths,” *IEEE Transactions on PAMI*, vol. 34, no. 10, pp. 1952–1965, 2012.

[6] H. Li, A. J. Yezzi, and L. D. Cohen, “3D multi-branch tubular surface and centerline extraction with 4D iterative key points,,” *In MICCAI, 2009*, pp. 1042–1050.

[7] R. Duits et al., “Image analysis and reconstruction using a wavelet transform constructed from a reducible representation of the Euclidean motion group,” *International Journal of Computer Vision*, vol. 79, no. 1, pp. 79–102, 2007.

[8] R. Duits et al., “Invertible orientation scores as an application of generalized wavelet theory,” *Pattern Recognition and Image Analysis*, vol. 17, no. 1, pp. 42–75, 2007.

[9] J. A. Sethian, “Fast marching methods,” *SIAM Review*, vol. 41, no. 2, pp. 199–235, 1999.

[10] A. F. Frangi, W. J. Niessen, K. L. Vincken, and M. A. Viergever, “Multiscale vessel enhancement filtering,” *In MICCAI*, vol. 1496, pp. 130–137, 1998.

[11] Erik Bekkers, R. Duits, B. Romeny, T. Berendschot, “A New Retinal Vessel Tracking Method Based on Orientation Scores,” *arXiv:1212.3530*, 2012.